2021 18th International Conference on Electrical Engineering, Computing Science and Automatic Control (CCE). Mexico City, Mexico. November 10-12, 2021

# *Ictal Periods Detection in Photoplethysmographic and Electrodermal Signals*

María Fernanda Ramírez-Peralta
*UPIITA*
*Instituto Politécnico Nacional*
Mexico City, Mexico
mfernanda.ramirezp@gmail.com

María Fernanda Romo-Fuentes
*UPIITA*
*Instituto Politécnico Nacional*
Mexico City, Mexico
mferomof@gmail.com

Blanca Tovar-Corona
*SEPI – UPIITA*
*Instituto Politécnico Nacional*
Mexico City, Mexico
bltovar@ipn.mx

Martin Arturo Silva-Ramírez
*Postgraduate professor UNAM*
*Hospital La Raza IMSS*
Mexico City, Mexico
neuro_marturosilva@yahoo.com

Laura Ivoone Garay-Jiménez
*SEPI – UPIITA*
*Instituto Politécnico Nacional*
Mexico City, Mexico
lgaray@ipn.mx

***Abstract*—The occurrence of an epileptic crisis can generate changes in the autonomous nervous system, given the relation between the zones in which an epileptic crisis generates and propagates, and the zones of the brain that control the involuntary responses of the body. Thus, an investigation aiming at identifying ictal periods in autonomous nervous system-controlled signals that can be, also, continuously recorded through a wearable device is proposed. Two signals are considered, electrodermal activity, obtained from the measurement of the galvanic skin response, and heart rate variability, derived from the analysis of the inter beat interval computed from the photoplethysmographic signal. A database of 11 subjects, composed by these two signals recorded simultaneously with electroencephalography is employed. Time and frequency-domain features were extracted from the electrodermal and heart rate variability signals by taking 4-minute segments previous to the beginning of a seizure as interictal, and 4-minute segments after as ictal, for training, and through a 4-minute windows with a 30-second slide segmentation for testing, while the electroencephalographic signal was taken as reference to obtain the tags for the ictal and interictal periods. The features were classified using a perceptron multilayer neural network trained with scaled conjugate gradient backpropagation algorithm, obtaining the following results, accuracy: 25.15%, recall: 97.49%, specificity: 0.44% precision: 24.86%, and F2 score: 60.12%.**

***Keywords—epilepsy, electrodermal activity, heart rate variability, ictal period detection, wearables***

## I. INTRODUCTION

The usage of wearables, which has become widespread nowadays, has driven research to find the possible solutions to everyday problems that can be addressed by analyzing the signals acquired through these devices. One of these addressed problems is the continuous monitoring of epileptic patients, and the identification of precursors and the beginning of ictal periods in a signal acquired from a patient, based on the changes these signals show given the alterations that the autonomous nervous system (ANS) suffers by the presence of an epileptic crisis.

Most of the research papers focused on the monitoring of epileptic patients by analyzing wearable acquired signals use: 1) the electrodermal activity (EDA), derived from the galvanic skin response (GSR), 2) heart rate variability (HRV) obtained from the analysis of the inter-beat interval (IBI) computed from the photoplethysmographic (PPG) signal, 3) movement derived from accelerometry (ACC) or 4) pulse oximetry (SpO2) computed, also, from PPG [1-4]. For this investigation, we will focus on EDA and HRV only.

In terms of the analysis of the EDA signal of epileptic patients, studies have shown that either by studying the signal itself [1,3] or studying it along with other signals [1], morphologic changes in the time and frequency domain extracted features can be observed when an ictal period begins and finishes, which allows to differentiate them.

For HRV, time and frequency domain extracted features correlate with the presence of an ictal period [5,6]. Furthermore, relevant changes in the autonomic regulation are related to sudden unexpected death in epilepsy (SUDEP) events reflected in the HRV signal [7].

Even though these changes have been observed, to our knowledge, there has not been an investigation that studies both EDA and HRV signals to identify ictal periods by using the electroencephalography (EEG) signal as a reference, namely, to acquire the tags needed for the classification. Thus, the following paper describes a methodology for extracting time and frequency domain characteristics from EDA and HRV and classifying them by a neural network. Signals go through two methods for segmentation: 1) For the training of the neural network, in which 4-minute segments are taken from the signal before and after the start of an ictal period, and 2) For the classification, a 4-minute windows with a 30-second slide from the signals.

This paper is divided into five sections. In section II the database employed in this research is described. In Section III the methodology for the analysis done to EEG signals to acquire the tags used in the classification and the process for feature extraction and classification for both EDA and HRV

978-1-6654-0029-9/21/$31.00 ©2021 IEEE

is presented. Then, in Section IV the analysis of the obtained results is developed, and the conclusions and discussion are presented in Section V.

## II. Materials

The database used in this project was developed by the Instrumentation and Signal Processing Laboratory (LIPS) in UPIITA-IPN and it has 11 recordings, each composed of six signals: EDA sampled at 4 Hz; PPG sampled at 64 Hz; IBI, obtained from PPG; Temperature; ACC; EEG sampled at 200 Hz and acquired through the 10/20 system.

The first five signals were recorded through the Empatica® e4 wearable device, and the EEG signal was acquired through a Comet-PLUS® Portable EEG-Recording & Review System from Grass Technologies®.

Signals from all recordings have a mean duration of 40 min and were acquired during an epileptic trigger-identifying session under the supervision of a specialist. Eight of the recorded patients had generalized epilepsy, one patient had frontal epilepsy and another, partial epilepsy. The ages of ten of the patients are in a range between 1 and 27 (14.3 ± 7.67) years, and the eleventh recording belongs to a 56-year-old patient.

## III. Methodology

### *A. Tags obtainment.*

The tags for the training and testing of the classifier are obtained from the EEG signal by applying the algorithm developed by Ramírez-Fuentes et al. [8]. This algorithm identifies the starts and endings of ictal periods based on the measurements of amplitude, frequency, and morphological analysis according to the clinical guides that specialists use as a reference to identify epileptic crises. As a result, a matrix with the size m*n was obtained, where m is the seconds of the EEG recording and n is the number of channels. The matrix was then processed to obtain a vector in which the initial and final seconds of the crisis are identified regardless of the channel, since we are only interested in the seconds in which an epileptic crisis occurs. The starting time and duration of the EEG, EDA and HRV signal recordings are compared, data is eliminated from either the crisis vector or the EDA and HRV signals, whichever starts before or lasts longer, so that they are tied in time. The obtained vector is handled in two ways: one for training and one for testing the classification algorithm.

For training, the second in which an ictal period starts is marked, the previous 4 min are considered interictal periods (tagged as 0), and the following 4 min are identified as ictal (tagged as 1). The seconds in which both the identified 4-minute ictal and interictal periods start and end are used in the feature extraction, which will be described in the following section. For testing, the vector is segmented into 4-minute windows with a 30-second slide, if there is at least one ictal period in the segment, it is identified as ictal (tagged as 1), otherwise, the segment is identified as interictal (tagged as 0).

For visualization of the three signals tied in time, in Fig. 1, 11 seconds of the recording from a 9-year-old patient diagnosed with generalized epilepsy are shown, in this segment there is an ictal period, identified through EEG, which lasts from seconds 2315 to 2326.

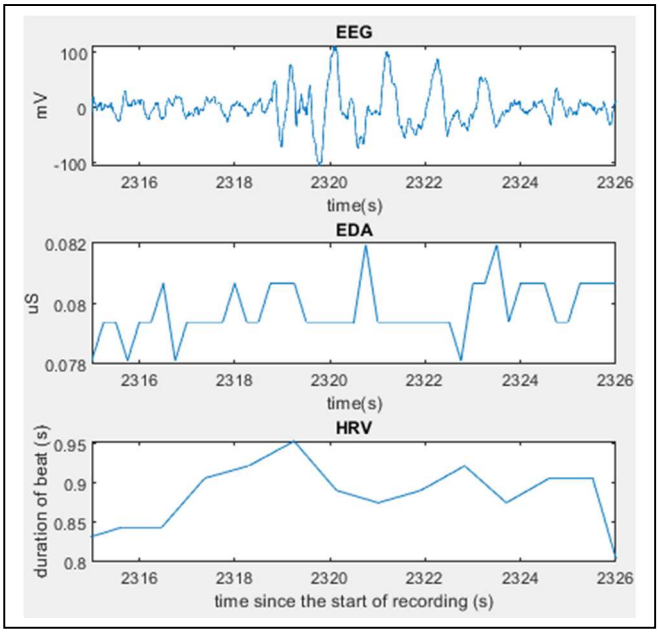


*Fig. 1. An identified ictal period in EEG, EDA and HRV during seconds 2315 to 2326 of the recording*

### *B. Feature extraction*

Feature extraction for both, EDA and HRV signals, is also done for classification and training. For training, the seconds in which the 4-minute interictal and ictal periods start and end, previously identified through EEG, and contained in the crisis vector are used. In both signals, these segments are identified and features in the time and frequency domain are extracted.

For EDA, the proposed methodology is summarized in the diagram in Fig. 2. First, an artifact correction was performed through a non-linear 5th order median filter, followed by computing the standard deviation of 15-second segments. If the value of each data point is higher than the value of its corresponding median filter value plus or minus 2.5 times the standard deviation of the segment, the sample is replaced by the mean of the previous and following two samples. Then, the following features are calculated.

*Time-domain features for EDA*

Statistical measures mean, variance, skewness, and kurtosis, along with sample entropy, minimum and maximum values, which are uniform and non-stimuli-markers dependent features were calculated as follows.

Mean, or first moment, is defined as:

$$\mu_1 = \frac{1}{N}\sum_{i=1}^{N} x_i \qquad \text{Eq. 1}$$

Where N is the number of data points in the analyzed segment, in this case, it is the length of the data vector corresponding to each window [9].

Variance, or second moment, is obtained as:

$$\mu_2 = \sigma^2 = \frac{1}{N}\sum_{i=1}^{N}(x_i - \mu_1)^2 \qquad \text{Eq. 2}$$

This measurement describes the width of the data distribution [9]. The standard deviation is the square root of the variance.

The third statistical moment is used to measure the asymmetry of a data distribution. The expression for this parameter is:

$$\mu_3 = \frac{1}{N}\sum_{i=1}^{N}(x_i - \mu_1)^3 \qquad \text{Eq. 3}$$

Then, the skewness coefficient is calculated as follows, from the second and third moment [9].

$$sk = \frac{\mu_3}{{\mu_2}^{3/2}} \qquad \text{Eq. 4}$$

The kurtosis coefficient reflects the shape of the probability distribution [9] from the fourth statistical moment defined as:

$$\mu_4 = \frac{1}{N}\sum_{i=1}^{N}(x_i - \mu_1)^4 \qquad \text{Eq. 5}$$

The expression for the kurtosis coefficient can also be understood as the fourth moment normalized with respect to the standard deviation, and is defined as:

$$\beta_2 = \frac{\frac{1}{N}\sum_{i=1}^{N}(x_i - \mu_1)^4}{{\mu_2}^2} \qquad \text{Eq. 6}$$

The sample entropy, that quantifies the variability of the data of a signal, or its degree of prediction [10,11] is defined as:

$$SampEn(m, r) = -ln\left(\frac{A_m}{B_m}\right) \qquad \text{Eq. 7}$$

For a data series of length N, sample segments of embedded dimension m per time interval **τ** are taken, with a tolerance r defined as 0.2 * (standard deviation).

With Am as:

$$d[X_{m+1}(i), X_{m+1}(j)] < r \qquad \text{Eq. 8}$$

And Bm as:

$$d[X_m(i), X_m(j)] < r \qquad \text{Eq. 9}$$

It is the negative of the natural logarithm of the probability that two groups of simultaneous points of length m have a distance less than r, and that the same happens for a vector of length m + 1. Indexes i, j are the position indexes.

These measurements are extracted without a reference signal such as EEG or ACC [12]. The window length proposal varies among authors, although windows' length between 1 and 5 s are suggested to pay attention to the fast changes component or electrodermal response (EDR) [13-15]. Furthermore, other authors recommend windows between 30 s and 5 min [12]. Thus, for this study, the 4-minute windows are selected.

*Frequency domain features for EDA*

All the extracted features are obtained from a sub-band analysis, taking the work of Posada-Quintero et al. as a reference. The identified sub-bands are: 0-0.045 Hz, 0.045 – 0.15 Hz, 0.15 – 0.25 Hz, 0.25 – 0.4 Hz, and 0.4 – 0.5 Hz [16].

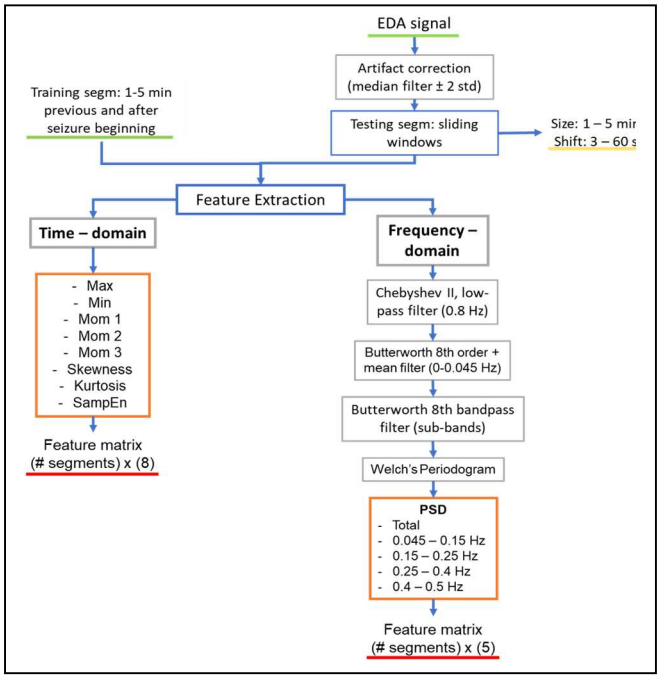


*Fig. 2. Feature extraction procedure for both training and testing stages of the EDA signal in time and frequency domains.*

First, a Chebyshev type II filter is applied at 0.8 Hz since it was confirmed with the frequency spectrum that there are no components in frequencies higher than 0.8 Hz. Then, a Butterworth 8th order filter is applied to separate each sub-band; first, a high-pass filter to eliminate the range of 0-0.045 Hz, along with a mean filter where the mean of every 4 data points is calculated and subtracted from the curve; and band-pass filters for the other bands. Afterward, Welch's Periodogram is performed for each segment and subband, with a Hanning window with 128 data points and 50% overlap. Finally, the power spectral density (PSD) is obtained with the trapezoid rule, a numerical integration method.

For HRV, an artifact correction is unnecessary since the wearable device employed to acquire the signal automatically removes the artifacts. The feature extraction for both training and testing in the time and frequency domain for the HRV signal is summarized in the diagram shown in Fig. 3 and the description of all the extracted features in both domains is described below.

*Time domain features for HRV*

For this signal, five statistical and one geometric time-domain features are extracted. These features being heart rate (HR), the standard deviation of the duration of successive heartbeats (SDRR), the square root of the duration of successive heartbeats (RMSSD), the number of successive heartbeats whose duration differ more than 50 ms (RR50), the RR50-Measurement in percentage (pRR50) and the HRV triangular index [5, 17, 18].

*Frequency domain features for HRV*

In this domain, all the features are computed from the Lomb-Scargle periodogram. The obtained periodogram is analyzed by dividing it into three sub-bands: Very low frequency (0.0033 to 0.04 Hz), low frequency (0.04 to 0.15 Hz), and high frequency (0.15 to 0.4 Hz). Thus, we have the following characteristics: the integral of the PSD in the very low frequency (VLF) band, the integral of PSD in the low frequency (LF) band, the integral of PSD in the high frequency (HF) band, the frequency with the highest peak in the low and high-frequency bands, and the LF/HF ratio [17, 18]. The trapezoidal rule is used to compute the integrals done per sub-band.

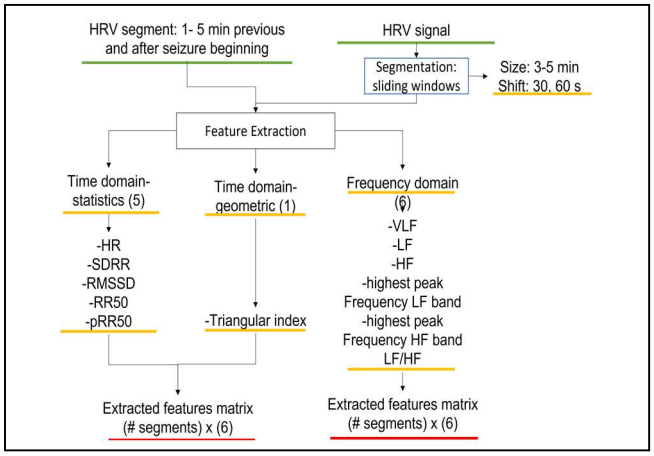


*Fig. 3. Feature extraction procedure for both training and testing stages of the HRV signal in time and frequency domains*

Initially, windows varying from 1 to 5 min were considered. However, an investigation made regarding clinical guidelines for short term segmentation of HRV [19] and tests made with the Lomb-Scargle periodogram showed that windows less than 3 minutes long do not provide the necessary information to study VLF and HF bands in some recordings from the analyzed database. Therefore, the signal is segmented in 3-to-5-minute windows to conduct tests.

## C. Classification

The use of a perceptron multilayer neural network (NN) is proposed, trained with a scaled conjugate gradient backpropagation algorithm to classify the segments into ictal or interictal periods. For the hidden layers, a sigmoid activation function, and for the output layer, a softmax function, were selected based on the comparison analysis of Nwankpa et al. [20].

For each segmentation and preprocessing method, a model of NN is obtained during training for EDA and HRV in time and frequency domains, separately, with a total of fifteen models for EDA and nine models for HRV in each domain. The process is shown in the block diagram of Fig. 4 and described below.

The features extracted from training segments of each signal, for each domain, are the NN inputs. Preliminarily, different segmentations of 1-5 min with shifts of 3-60 s for EDA, and 3-5 min with shifts of 30-60 s for HRV, were proposed and evaluated, in addition with three methods used to preprocess the features previous to the NN, described as follows:

1. Normalization of the data considering the maximum absolute value for each feature, for each record.
2. Normalization of the data, and application of the Principal Component Analysis (PCA) to preserve those features that contribute at least 95% of the total variance for each principal component.
3. Since specific segments were taken, few features were obtained for training, then, the Bootstrap Aggregation (Bagging) method was proposed to increase data points. The algorithm takes data randomly with replacement and obtains the mean as the new data point. This method is widely used in learning ensembles, along with decision trees (Tree Bagger) [21,22] and, in some applications, it has shown to improve the performance of NN [23]. This algorithm is applied after normalization and PCA, to ictal and interictal data points separately.

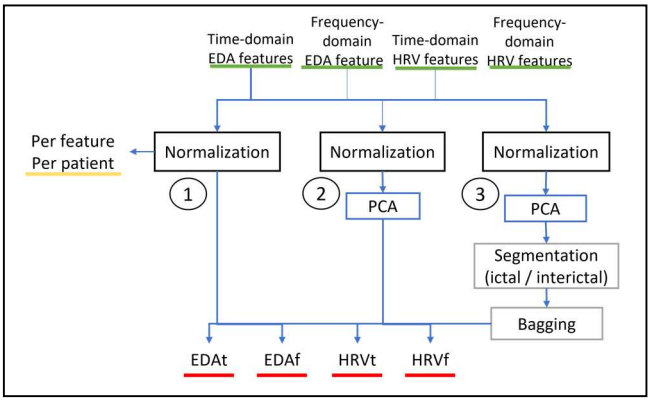


*Fig. 4. Classification models for both signals in time and frequency domain*

Each model of NN was evaluated using Machine Learning metrics, such as accuracy, recall, precision, sensitivity, specificity, and Fβ score, during the training stage using the first described tagging and segmentation methodology, and finally, during testing using the second one. For this, the ictal data are considered as positives, and the interictal as negatives.

# IV. Results and Discussion

From all the evaluation metrics considered, accuracy was used to determine the window length, and recall was used to determine the preprocessing method.

According to the performance evaluation, the 4-minute windows with a 30-second shift provided better results. Moreover, for each domain for each signal, a method of preprocessing of the features was required. Normalization and PCA model for EDA in time and frequency domains and HRV in frequency-domain, meanwhile, for HRV in the time domain, the Bagging method improved the performance for 4-minute models specifically.

The evaluation results are shown in Table 1, where the maximum accuracy and recall metrics for each method were obtained as the mean corresponding to all the shifts for the same window length, for all recordings from all patients. The

standard deviation for each metric of interest indicates that the shift does not affect the performance for the same window length.

The final classification decision was made by first, comparing the NN outputs for each signal in both domains, for each signal, the frequency-domain response is preferred. Then the output of both signals is compared, if they differ, the final output value is taken as the EDA-freq NN output since the performance of this model presented uniformity regardless of the segmentation, shifting, and recording used for testing. The proposed model provides the following results: accuracy: 25.15%, recall: 97.49%, specificity: 0.44% precision: 24.86%, and F2 score: 60.12%.

*Table 1. Metrics of interest for evaluation of neural networks*

| Features | Window length | Metric | Data preprocessing (training) | | |
|---|---|---|---|---|---|
| | | | Norm | Norm – PCA | Norm – PCA – Bagg |
| EDA freq | 5 min | **Accuracy** | Mean: 52.72 % Std: 0.025 | Mean: 45.47 % Std: 0.1065 | Mean: 28.10 % Std: 0.0139 |
| | 1 – 4 min | **Recall** | Mean: 69.76 % Std: 0.0472 | Mean: **93.69 %** Std: 0.0215 | Mean: 100 % Std: 0.0001 |
| EDA time | 5 min | **Accuracy** | Mean: 64.30 % Std: 0.1288 | Mean: 40.66 % Std: 0.787 | Mean: 27.74 % Std: 0.0144 |
| | 1 – 4 min | **Recall** | Mean: 62.73 % Std: 0.1604 | Mean: **97.70 %** Std: 0.193 | Mean: 98.89 % Std: 0.0099 |
| HRV freq | 3 min | **Accuracy** | Mean: 38.65 % Std: 0.0016 | Mean: 77.23 % Std: 0.0004 | Mean: 74.69 % Std: 0.0145 |
| | 4 min | **Recall** | Mean: 44.18 % Std: 0.0787 | Mean: **100 %** Std: 0.000 | Mean: 57.84 % Std: 0.1636 |
| HRV time | 4 min | **Accuracy** | Mean: 41.45 % Std: 0.281 | Mean: 74.37 % Std: 0.0145 | Mean: 31.96 % Std: 0.0067 |
| | 4 min | **Recall** | Mean: 61.61 % Std: 0.0312 | Mean: 6.71 % Std: 0.0451 | Mean: **81.05 %** Std: 0.0121 |

Some studies performed using long-duration recordings have determined that the recovery time of EDA and HRV signals after the occurrence of an epileptic seizure is variable, from several minutes to hours [3,12,15,24]. Hence, to correctly characterize interictal periods it is recommended that the signals return to their basal state, ensuring that the ictal period has completely ended. This characterization will ensure higher values of accuracy, specificity and precision, since these metrics take into account the classification of interictal periods.

With the feature extraction and classification process described in this paper, a user guide interface using the MATLAB® R2020b software was developed, this interface provides the identification of ictal periods and an evaluation of the results by comparing the output with the tags obtained from EEG analysis.

In Fig. 5, the EEG, HRV, and EDA signals of a 9-year-old patient diagnosed with generalized epilepsy are used in the developed interface. As a result, the graphs in a) show the ictal and interictal classification obtained for the EDA and HRV signals, while the graphs in b) show the expected output vs. the obtained output result of the same classification process.

## V. Conclusions

The presented methodology has proven efficient for ictal periods detection with a true positive rate of 97%. However, the interictal periods' detection is not equally accurate, mainly because the severity of the pathology, age of the patient, and other factors, such as possible precursors affect the intensity and duration of the ictal events.

Furthermore, the effects in EDA and HRV may last from several minutes to hours, and this could mean that the interictal periods defined in short- length recordings may still present the effects of previous and following ictal periods, then, those interictal periods would be classified as ictal. Therefore, it is expected to have a low true negative rate and a low accuracy value, thus further studies should be done. The analysis of long duration records (hours or days long) that would allow a more in-depth study of the effects of ictal events to differentiate from interictal periods more accurately and even evaluate whether precursors to seizures are present in EDA and HRV, is suggested for future investigations.

In general, the use of PCA resulted in an improvement to the models compared to only normalizing the data, given that the preserved features were representative for each signal. In specific segmentations, bagging also contributed to enhancing the NN performance, especially in HRV models. Although bagging is a method to avoid overfitting, in some cases, perhaps due to the nature of interictal data, it worsened the performance of the classifier.

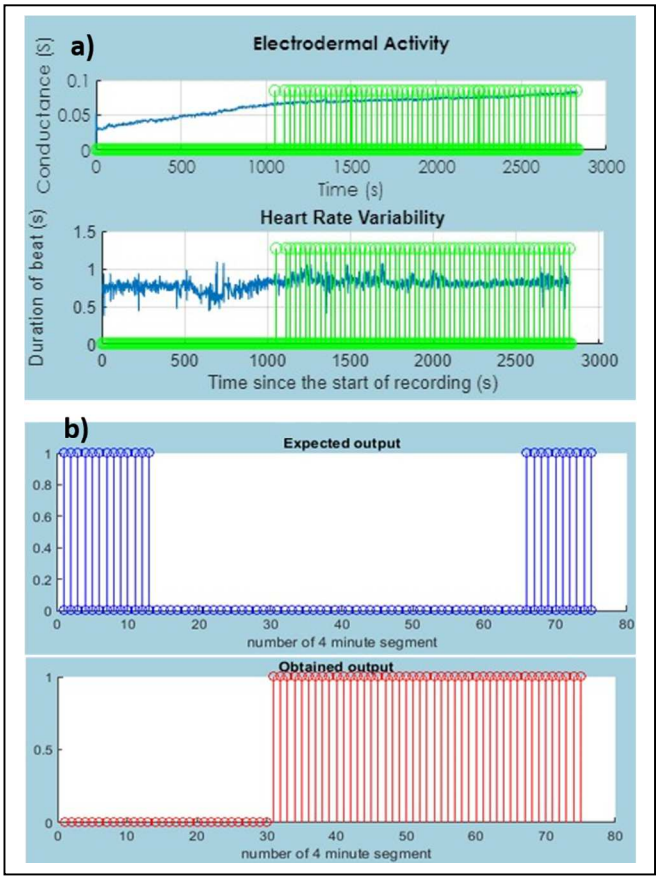


*Fig. 5. Classification results. a) The identified ictal and interictal periods corresponding to the analysis of the EDA and HRV signals are shown. b) A comparison between the expected output and the obtained output per 4-minute segment*

However, this technique should be considered for long-duration recordings, where these periods could be more accurately characterized.

It must be noted that, at first, different segmentations were considered for both signals in both domains, after different tests were made it was found that the segmentation could be done with 4-minute windows with a 30-second slide for all cases, nonetheless, different models provided better results for each signal and domain, therefore classification of all the extracted features was not done using a single neural network. It is suggested that this could be possible in future research by analyzing long duration records in which it is possible to better characterize the data.

Additionally, Tree Bagger ensembles and SVM models were also proposed and evaluated for comparison. The Tree-Bagger was proposed with 30 decision trees and a minimum Leaf Size of 5, evaluated through the out-of-the-bag prediction and pruning based on Gini's impurity; the SVM models were set with a radial kernel. The maximum accuracy and recall for these models for the 4-min segments were for Tree Bagger 47.5% and 100%, respectively, and for the SVM model 28.32% and 100%. However, the other metrics for both classifiers were 0 or NaN. Therefore, the perceptron multilayer neural network has shown a logical and more stable response than the Tree Bagger and SVM models considered for this application.

## ACKNOWLEDGMENT

Authors thank for the support through project SIP20210855.

## REFERENCES

[1] D. Cogan, J. Birjandtalab, M. Nourani, J. Harvey, y V. Nagaraddi, "Multi-Biosignal Analysis for Epileptic Seizure Monitoring, Int. J. Neur. Syst., vol. 27, núm. 01, p. 1650031, feb. 2017, doi: 10.1142/S0129065716500313.

[2] Hong, K.H.; Lee, S.M.; Lim, Y.G.; Park, K.S. Measuring skin conductance over clothes. Med. Biol. Eng. Comput.2012,50, 1155–1161.

[3] G. Regaliaa, F. Onorati, M. Lai, C. Caborni, y R. W. Picard, "Multimodal wrist-worn devices for seizure detection and advancing research: Focus on the Empatica wristbands", Epilepsy Research, vol. 153, pp. 79–82, jul. 2019, doi: 10.1016/j.eplepsyres.2019.02.007.

[4] R. Olival-Lima y H.F. Silveira, "Autonoumous Nervous System biosignal processing via EDA and HRV from a wearable device", 2018. [Online]. Available at: https://www.semanticscholar.org/paper/Autonoumous-Nervous-System-biosignalprocessing-via-Lima/62f065e7bbec84ab7f6880efa80e0e5e80bf9aba. [Accessed: 21-mar-2020]

[5] M. Safavi et al., «Analysis of Cardiovascular Changes Caused by Epileptic Seizures in Human Photoplethysmogram Signal». Cornell University, 2019, Accessed: dic. 02, 2020. [Online]. Available at: https://arxiv.org/pdf/1912.05083.pdf.

[6] J. Jeppesen, S. Beniczky, P. Johansen, P. Sidenius, y A. Fuglsang-Frederiksen, «Detection of epileptic seizures with a modified heart rate variability algorithm based on Lorenz plot», Seizure, vol. 24, pp. 1-7, ene. 2015, doi: 10.1016/j.seizure.2014.11.004

[7] K. A. Myers et al., «Heart rate variability in epilepsy: A potential biomarker of sudden unexpected death in epilepsy risk», Epilepsia, vol. 59, no 7, pp. 1372- 1380, jul. 2018, doi: 10.1111/epi.14438.

[8] C. A. Ramírez-Fuentes et al., «A Methodology for the Automatic Identification and Classification of EEG waves based on Clinical Guidelines», Proceedings of the 9th International Multi-Conference on Complexity, Informatics and Cybernetics (IMCIC), Vol. II, 2018, ISBN: 978-1-941763-70-4

[9] «Moment Statistics». University of Houston, Accessed: dic. 17, 2020. [Online]. Available: https://uh.edu/~odonnell/econ2370/moment.pdf.

[10] S. Guardiola, «Análisis de señales biomédicas para la detección del nivel de estrés/relajación de conductores», Universitat Politècnica de València, Valencia, Spain, 2016.

[11] P. Castiglioni et al., «Assessing Sample Entropy of physiological signals by the norm component matrix algorithm: Application on muscular signals during isometric contraction», 35th Annual International Conference of the IEEE Engineering in Medicine and Biology Society (EMBC), jul. 2013, pp. 5053-5056, doi: 10.1109/EMBC.2013.6610684.

[12] S. Vieluf et al., «Autonomic nervous system changes detected with peripheral sensors in the setting of epileptic seizures», Sci Rep, vol. 10, n.o 1, p. 11560, dic. 2020, doi: 10.1038/s41598-020-68434-z

[13] M. Kołodziej, P. Tarnowski, A. Majkowski, y R. J. Rak, «Electrodermal activity measurements for detection of emotional arousal», 2019, doi: 10.24425/BPASTS.2019.130190.

[14] F. Hernando Gallego, D. Luengo, y A. Artés Rodríguez, «Feature Extraction of Galvanic Skin Responses by Non-Negative Sparse Deconvolution», IEEE Journal of Biomedical and Health Informatics, vol. PP, pp. 1-1, dic. 2017, doi: 10.1109/JBHI.2017.2780252.

[15] M. Benedek y C. Kaernbach, «A continuous measure of phasic electrodermal activity», J Neurosci Methods, vol. 190, n.o 1-5, pp. 80-91, jun. 2010, doi: 10.1016/j.jneumeth.2010.04.028.

[16] H. F. Posada-Quintero y K. H. Chon, «Innovations in Electrodermal Activity Data Collection and Signal Processing: A Systematic Review», Sensors, vol. 20, n.o 2, p. 479, ene. 2020, doi: 10.3390/s20020479.

[17] G. Giannakakis, M. Tsiknakis, y P. Vorgia, «Focal epileptic seizures anticipation based on patterns of heart rate variability parameters», Computer Methods and Programs in Biomedicine, vol. 178, pp. 123-133, sep. 2019, doi: 10.1016/j.cmpb.2019.05.032.

[18] M. Yilmaz, H. Kayancicek, y Y. Cekici, «Heart rate variability: Highlights from hidden signals», J Integr Cardiol, vol. 4, n.o 5, 2018, doi: 10.15761/JIC.1000258

[19] F. Shaffer y J. P. Ginsberg, «An Overview of Heart Rate Variability Metrics and Norms», *Front. Public Health*, vol. 5, p. 258, sep. 2017, doi: 10.3389/fpubh.2017.00258.

[20] C. Nwankpa, W. Ijomah, A. Gachagan, y S. Marshall, «Activation Functions: Comparison of trends in Practice and Research for Deep Learning», *arXiv:1811.03378 [cs]*, nov. 2018, Accessed: may 17, 2021. [Online]. Available at: http://arxiv.org/abs/1811.03378

[21] L. I. Kuncheva, «Ensamble Methods. Bagging», en Combining pattern classifiers: methods and algorithms, Second edition., Hoboken, NJ: Wiley, 2014, pp. 186-190.

[22] J. Brownlee, «Ensable Algorithms», en Master Machine Learning Algorithms: Discover How They Work and Implement Them From Scratch, Machine Learning Mastery, 2016, pp. 126-149.

[23] M. F. Tahir, Tehzeeb-ul-Hassan, y M. A. Saqib, «Optimal scheduling of electrical power in energy-deficient scenarios using artificial neural network and Bootstrap aggregating», International Journal of Electrical Power & Energy Systems, vol. 83, pp. 49-57, dic. 2016, doi: 10.1016/j.ijepes.2016.03.046.

[24] A. Zsom *et al.*, «Ictal autonomic activity recorded via wearable-sensors plus machine learning can discriminate epileptic and psychogenic nonepileptic seizures», en *2019 41st Annual International Conference of the IEEE Engineering in Medicine and Biology Society (EMBC)*, Berlin, Germany, jul. 2019, pp. 3502-3506. doi: 10.1109/EMBC.2019.8857552.